Kinetic Study of the Reaction of OH with H_2 and D_2 from 250 to 1050 K

A. R. Ravishankara,* J. M. Nicovich, R. L. Thompson, and F. P. Tully†

Molecular Sciences Branch, Engineering Experiment Station, Georgia Institute of Technology, Atlanta, Georgia 30332
(Received: January 30, 1981; In Final Form: April 20, 1981)

Absolute rate coefficients for the reactions OH + H_2 → H_2O + H (k_1) and OH + D_2 → DHO + D (k_2) have been measured between 250 and 1050 K by using the flash photolysis–resonance fluorescence technique. The adaptation of the flash photolysis–resonance fluorescence technique to high-temperature studies is described. The measured values of k_1 and k_2 exhibit non-Arrhenius behavior. k_1 and k_2 are best described by three-parameter functions, $k_1(T) = (4.12 \times 10^{-19})T^{2.44} \exp(-1281/T)$ cm^3 molecule^{-1} s^{-1} and $k_2(T) = (4.37 \times 10^{-15})T^{1.18} \exp(-2332/T)$ cm^3 molecule^{-1} s^{-1} over the entire temperature range 250–1050 K. Alternatively, at low temperatures k_1 and k_2 can be described by Arrhenius expressions, $k_1(T) = (4.9 \pm 0.5) \times 10^{-12} \exp[-(1.99 \pm 0.34) \times 10^3/T]$ cm^3 molecule^{-1} s^{-1} for $250 < T < 400$ K and $k_2(T) = (1.21 \pm 0.52) \times 10^{-11} \exp[-(2.67 \pm 0.15) \times 10^3/T]$ cm^3 molecule^{-1} s^{-1} for $250 < T < 470$ K. The results are compared with theoretical calculations based on an ab initio potential energy surface for reaction 1.

Introduction

The high-temperature kinetic data needed for combustion modeling has been mainly derived from shock-tube and flame studies. In these experiments, the accuracy of the obtained rate data is dependent on the degree of understanding of the chemistry involved in the system that is studied. In many cases it has been found that the extrapolation of the derived high-temperature ($T > 1000$ K) data to low temperatures ($T < 500$ K) yields rate coefficients which disagree with the results of direct low-temperature measurements. It has recently been recognized that this discrepancy could be due either to non-Arrhenius behavior[1-3] of the reaction under study or to systematic errors in the high-temperature data. To fully understand the variation of rate coefficients with temperature in the intermediate temperature range, i.e., $298 < T < 1000$ K, one needs direct experimental measurements of elementary reaction rate coefficients. This need has recently encouraged adaptation of proven low-temperature kinetic techniques to intermediate- and high-temperature studies. The developments have provided techniques which can directly measure the rate coefficient for an elementary reaction over a wide temperature range, thus minimizing the likelihood of relative systematic errors. In parallel to these experimental developments, advances have been made in theoretical computation of elementary reaction rate coefficients.[4,5] The transition-state theory has been improved to a point where quite rigorous calculations of thermal rate coefficients can be carried out.[6] The capacity to calculate rate coefficients can be principally attributed to the availability of calculated ab initio potential energy surfaces for many atom–diatom reactions and even four-atom systems such as OH + H_2.[7]

We have recently adapted the conventional technique of flash photolysis–resonance fluorescence to measure OH reaction rate coefficients at temperatures above 1000 K.[8,9] The rate coefficient for reaction 1 was measured in the

$$\mathrm{OH} + \mathrm{H_2} \xrightarrow{k_1} \mathrm{H_2O} + \mathrm{H} \qquad (1)$$

temperature range 298–992 K, and the ln k_1 vs. $1/T$ plot was found to be nonlinear.[8] Since our measurement of k_1, an ab initio calculation of the potential energy surface for this reaction,[7] as well as a transition-state theory calculation[5] of k_1 which utilized this surface, have been reported. The potential energy surface for reaction 2 should be

$$\mathrm{OH} + \mathrm{D_2} \xrightarrow{k_2} \mathrm{DHO} + \mathrm{D} \qquad (2)$$

identical with that for reaction 1 within the Born–Oppenheimer approximation; comparison of measured values with calculated values of k_2 would thus constitute a direct test of the theoretical computations. Also, the effect of isotopic substitution on the curvature of Arrhenius plots would be probed. Therefore, we have measured k_2 over the temperature range 250–1050 K and have extended our earlier measurements of k_1 to span the same temperature range.

Experimental Section

The utilization of the flash photolysis–resonance fluorescence (FP–RF) technique in studies of OH radical reaction kinetics at temperatures below 500 K is amply described in the literature.[10,11] We have recently adapted this technique for studies at temperatures up to ~1100 K. In this paper we describe in detail the system modifications which are required for high-temperature operation.

The primary difficulty in using the FP–RF technique at high temperatures is the maintainance of good OH detection sensitivity while using a reactor which can be

†Applied Physics Division, Sandia National Laboratories, Livermore, CA 94550.

(1) F. Dryer, D. Naegeli, and I. Glassman, *Combust. Flame*, **17**, 270 (1970).
(2) R. Zellner, *J. Phys. Chem.*, **83**, 18 (1979).
(3) W. C. Gardiner, Jr., *Acc. Chem. Res.*, **10**, 326 (1977).
(4) D. M. Golden, *J. Phys. Chem.*, **83**, 109 (1979), and references therein.
(5) G. C. Schatz and S. P. Walch, *J. Chem. Phys.*, **72**, 776 (1980).
(6) B. C. Garrett, D. G. Truhlar, R. S. Grev, and A. Magnuson, *J. Phys. Chem.*, **84**, 1730 (1980).
(7) S. P. Walch and T. H. Dunning, *J. Chem. Phys.*, **72**, 1303 (1980).
(8) F. P. Tully and A. R. Ravishankara, *J. Phys. Chem.*, **84**, 3126 (1980).
(9) F. P. Tully, A. R. Ravishankara, R. L. Thompson, J. M. Nocovich, R. C. Shah, N. M. Kreutter, and P. H. Wine, *J. Phys. Chem.*, **85**, 2262 (1981).
(10) (a) D. D. Davis, S. Fischer, and R. Schiff, *J. Chem. Phys.*, **59**, 628 (1974); (b) A. R. Ravishankara, P. H. Wine, and A. O. Langford, *ibid.*, **70**, 984 (1979); (c) A. R. Ravishankara, G. Smith, R. T. Watson, and D. D. Davis, *J. Phys. Chem.*, **81**, 2220 (1977).
(11) P. H. Wine, N. M. Kreutter, and A. R. Ravishankara, *J. Phys. Chem.*, **83**, 3191 (1979).

0022-3654/81/2085-2498$01.25/0

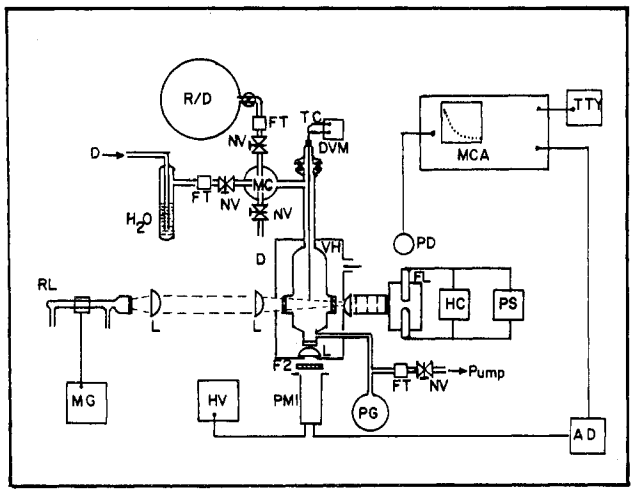

Figure 1. Schematic diagram of the high-temperature flash photolysis–resonance fluorescence apparatus: (AD) amplifier discriminator; (D) diluent gas; (DVM) digital voltmeter; (F2) 309.5-nm band-pass filter; (FL) flash lamp; (FT) flow transducer; (HC) high-voltage capacitor; (HV) high voltage; (L) lens; (MC) mixing chamber; (MCA) multichannel analyzer; (MG) microwave generator; (NV) needle valve; (PD) photodiode; (PG) pressure gauge; (PM1) photomultiplier RCA 8850; (PS) high-voltage power supply; (R/D) reactant/diluent gas; (RL) resonance lamp; (TC) thermocouple; (TTY) teletype; (VH) vacuum housing.

operated at these temperatures. A considerable amount of time was spent experimenting with various cell designs, cell materials, focusing optics, and light baffle arrangements in order to maximize OH detection sensitivity under high-temperature conditions. The final apparatus configuration is shown in Figure 1. The principal system components are (1) a thermostated reaction cell centered in a vacuum housing, (2) a spark discharge flash lamp perpendicular to one face of the cell, (3) a CW OH resonance lamp perpendicular to the photolysis beam, (4) a band-pass filter/photomultiplier combination for monitoring OH resonance fluorescence emitted perpendicular to both the photolysis and resonance radiation beams, and (5) a signal averager and fast photon counting electronics.

The reactor is constructed entirely out of quartz. Five highly polished Suprasil windows are fused to the cell by using quartz tape. The cell is coated with graphite on its outer surface. Once baked, the graphite bonds well with the quartz surface. The black graphite coating serves two purposes: (1) it lowers the detection of scattered radiation, and (2) it forms a good thermally conductive surface which helps avoid "hot spots". The cell is heated by using tantalum wire windings which are contained inside ceramic tubes. The heaters are powered by a constant-voltage power supply, and the temperature is controlled by changing the applied voltage with Variacs. The cell and the insulated heaters are wrapped with at least five layers of thin stainless-steel radiation shields to minimize radiative heat loss. A chromel–alumel thermocouple is attached to the outer surface of the reactor primarily to monitor the temperature of the cell during heating and cooling periods. The temperature of the gas inside the reactor is directly measured with a thermocouple which is inserted into the reactor. In preliminary characterization experiments the temperature differential between the upper and lower portions of the reaction zone (maximum length $\approx$ 2 cm) was found to be <5 K at 1000 K and negligible at 500 K. The bottom window (the fluorescence port located ~5 cm below the active volume) was measured to be ~15 K cooler than the active volume at 1000 K when the gases were flowing through the cell. Therefore, it may be confidently stated that at 1000 K the temperature in the active zone is constant to within 5 K and known to better than 10 K.

The utilization of the quartz reactor (in place of our previous Pyrex reactor) resulted in a large increase in the background scattered resonance lamp radiation. To overcome this problem, two modifications were carried out. (a) The microwave discharge lamp, the source of resonance radiation, was moved ~80 cm away from the cell. A 5-cm diameter quartz convex lens was placed ~20 cm from the discharge to collect the radiation and render it nearly parallel. A second 5-cm diameter quartz lens located ~15 cm from the center of the reactor focused this parallel beam onto the far port of the reactor. This configuration not only enabled almost all resonance radiation to pass only through the cell windows but also increased its flux at the active volume. (b) The photon counting electronics were improved to count linearly up to ~3 MHz. Typically, the measured background count rate ranged from 100 to 200 kHz. (It should be pointed out that the photon flux level used in this work is much higher than that characteristically employed in most previous FP–RF studies, where emphasis is placed on reducing the background rate to a very low value, often at the expense of decreasing the resonance radiation flux.) The output of the N_2 flash lamp was collimated by a set of baffles and then rendered approximately parallel by a pitch polished Suprasil lens, ensuring that all flash radiation exited only through the windows. Additional lenses were employed to collect the OH fluorescence from the center of the cell and then focus it onto the photocathode of an RCA 8850 photomultiplier tube. Use of this latter lens set resulted in increases in both fluorescence signal and background light with a large improvement in signal-to-noise ratio.

The sensitivity of the apparatus toward OH detection was determined by using a method previously described in detail.[11] The results of actinometry indicate that $\sim 1 \times 10^9$ OH per cm^3 could be detected (signal/noise = 1) with an integration time of 1×10^{-3} s, and under the typical experimental conditions (flash energy = 70–200 J, 50–150 mtorr of H_2O, 100 torr of Ar) employed in the present study, the initial OH concentrations ranged from 1×10^{10} to 1×10^{11} cm^{-3}. Here, signal-to-noise is defined to be signal above the background divided by the square root of background. This definition holds since the photon detection was truly statistical and the noise, i.e., fluctuations divided by the square root of the mean value of background, improved as the square root of the integration time (i.e., number of sweeps). It was found that, as long as the reactor was kept clean, the measured signal for a given OH concentration did not deteriorate significantly with increases in temperature.

All experiments were carried out by using Ar diluent gas (~100 torr) under pseudo-first-order kinetic conditions with $[H_2]$ and $[D_2]$ in large excess over [OH]. ($[H_2]/[OH]$ and $[D_2]/[OH]$ ratios were always greater than 1000. $[H_2]$ ranged from $\sim 2 \times 10^{13}$ to 2×10^{17} cm^{-3} and $[D_2]$ ranged from $\sim 2 \times 10^{13}$ to 1×10^{18} cm^{-3}.) OH radicals were produced by flash photolysis of H_2O at wavelengths between the Suprasil cutoff at 165 nm and the onset of continuum absorption at 185 nm (flash duration $\leq$ 50 μs). Following the flash, weakly focused OH resonance lamp radiation continuously excited a small fraction of the OH in the reactor to the electronically excited $A^2\Sigma^+$ state; the resultant (0,0) band $A \rightarrow X$ fluorescence emanating in the direction perpendicular to both the resonance excitation and photolysis beams was collected by the lens set and focused onto a photomultiplier fitted with a band-pass filter (309.5-nm peak transmission, 10-nm fwhm). Signals

TABLE I: Rate Coefficient vs. Temperature for Reaction 1, $OH + H_2 \rightarrow H_2O + H$

temp, K	k_1, cm^3 molecule^{-1} s^{-1}	temp, K	k_1, cm^3 molecule^{-1} s^{-1}
250	$(1.69 \pm 0.14) \times 10^{-15}$	356	$(1.83 \pm 0.08) \times 10^{-14}$
265	$(2.67 \pm 0.37) \times 10^{-15}$	366	$(2.02 \pm 0.21) \times 10^{-14}$
282	$(4.14 \pm 0.30) \times 10^{-15}$	396	$(3.32 \pm 0.11) \times 10^{-14}$
295	$(5.64 \pm 0.60) \times 10^{-15}$	960	$(2.40 \pm 0.25) \times 10^{-12}$
333	$(1.28 \pm 0.05) \times 10^{-14}$	1050	$(3.20 \pm 0.44) \times 10^{-12}$

TABLE II: Rate Coefficient vs. Temperature for Reaction 2, $OH + D_2 \rightarrow DHO + H$

temp, K	k_2, cm^3 molecule^{-1} s^{-1}	temp, K	k_2, cm^3 molecule^{-1} s^{-1}
250	$(3.16 \pm 0.25) \times 10^{-16}$	525	$(8.86 \pm 0.85) \times 10^{-14}$
268	$(5.00 \pm 0.57) \times 10^{-16}$	572	$(1.74 \pm 0.06) \times 10^{-13}$
298	$(1.83 \pm 0.12) \times 10^{-15}$	605	$(1.61 \pm 0.10) \times 10^{-13}$
336	$(3.98 \pm 0.17) \times 10^{-15}$	617	$(2.31 \pm 0.04) \times 10^{-13}$
356	$(6.03 \pm 0.36) \times 10^{-15}$	664	$(3.47 \pm 0.20) \times 10^{-13}$
366	$(7.07 \pm 0.71) \times 10^{-15}$	752	$(4.82 \pm 0.21) \times 10^{-13}$
380	$(1.07 \pm 0.05) \times 10^{-14}$	788	$(5.93 \pm 0.34) \times 10^{-13}$
398	$(1.18 \pm 0.18) \times 10^{-14}$	820	$(7.8 \pm 1.1) \times 10^{-13}$
438	$(3.07 \pm 0.23) \times 10^{-14}$	932	$(1.11 \pm 0.03) \times 10^{-12}$
449	$(3.35 \pm 0.14) \times 10^{-14}$	960	$(1.28 \pm 0.11) \times 10^{-12}$
471	$(4.81 \pm 0.37) \times 10^{-14}$	1050	$(1.61 \pm 0.25) \times 10^{-12}$

obtained by photon counting were fed into a signal averager operated in the multichannel scaling mode. For each decay rate measured, sufficient flashes (50–1000) were averaged to construct a well-defined temporal profile over at least a factor of 20 variation in [OH]. The time segments used varied from 100 μs to 1 ms, and signal-to-noise of at least 40 was attained for each decay curve.

All experiments were carried out under "slow flow" conditions. The flow rate through the reactor was such that each photolysis flash encountered a fresh reaction mixture (photolysis repetition rate $\approx$ 0.3 Hz). At temperatures greater than 270 K, H_2 (D_2) was flowed from a 12-L source bulb containing H_2 (D_2)/argon mixture, and the water mixture was generated by bubbling argon gas at 800 torr through distilled water at room temperature. The H_2 (D_2)/argon mixture, the H_2O/argon mixture, and additional diluent gas (Ar) were mixed before entering the reaction cell. The concentration of each component in the reaction mixture was determined from measurements of the appropriate mass flow rates (measured by using calibrated mass flowmeters) and the total pressure (usually 100 torr). At temperatures below 270 K, the amounts of H_2 and D_2 needed to carry out the experiments were so large that pure H_2 or D_2 would have been needed in the source bulb. We therefore prepared a large amount of an H_2 (D_2)/diluent gas mixture in a ~40-L volume and flowed it directly into the reactor after mixing it with a small amount of the H_2O/diluent gas mixture. This procedure avoided any possible flowmeter calibration errors.

The gases used in this study had the following stated purities: Ar > 99.9995%, H_2 > 99.9999%, D_2 > 99.96%. All gases were obtained from Matheson Gas Products. The D_2 mixture had less than 1 ppm of organics (mainly as CH_4) and had an isotopic purity of 99.5%. H_2 and D_2 were passed through liquid-nitrogen traps filled with glass beads before use to remove any condensable organics. Ar was used as supplied.

Results

All experiments were carried out under pseudo-first-order conditions with $[H_2]$ or $[D_2] \gg [OH]$. Therefore, in the absence of complicating secondary reactions, the temporal profile of [OH] is given by the equation

$$\ln \{[OH]_0/[OH]_t\} = (k_x[X] + k_d)t = k't$$

where X is either H_2 or D_2, k_x is the bimolecular rate constant of interest, k_d is the first-order rate constant for the loss of OH in the absence of X, and k' is the measured pseudo-first-order rate constant. [OH] decays were observed to be exponential for at least three $1/e$ times as typified by the data shown in Figure 2; the observation of exponential [OH] decays validates the existence of first-order conditions. At each temperature, the [OH] decay

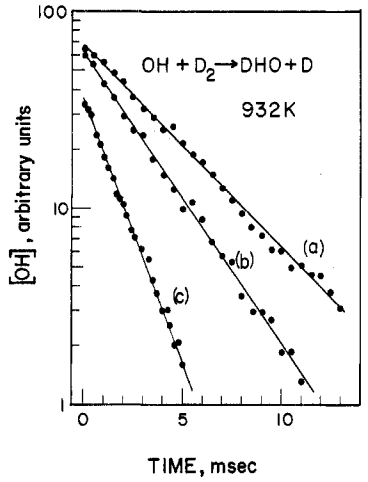

Figure 2. Typical [OH] temporal profile following flash photolysis of $H_2O/D_2/Ar$ mixture. Experimental conditions: T = 932 K; P = 100 torr (Ar); flash energy = 80 J; $[H_2O]$ = 70 mtorr; Concentration of D_2 in molecules cm^{-3}; (a) 1.08×10^{14}, (b) 2.09×10^{14}, (c) 4.88×10^{14}.

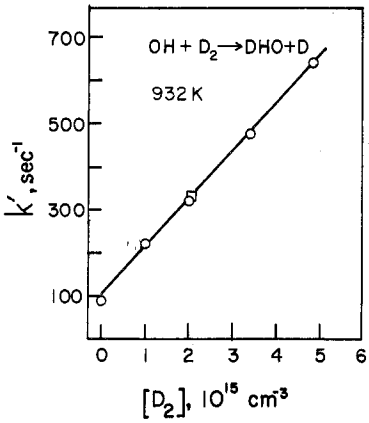

Figure 3. Plot of the pseudo-first-order rate constant vs. $[D_2]$ at 932 K. Solid line was obtained by linear least-squares analysis of k' vs. $[D_2]$ data. Flash energy; (O) 80 and (□) 200 J.

TABLE III: Summary of Rate-Constant Data for Reaction 1, OH + H_2 → H_2O + H

$k_1(298) \times 10^{15}$, cm^3 $molecule^{-1}$ s^{-1}	$10^{12}A$, cm^3 $molecule^{-1}$ s^{-1}	E/R, K	temp range, K	technique[a]	ref
7.1 ± 1.7				DF-RF	12
6.5 ± 0.35				DF-ESR	13
7.9	$6.76^{+1.76}_{-1.39}$	2030 ± 91	300-500	FP-RA	17
7.1 ± 1.1				FP-RF	14
7.6	*b*	*b*	298-745	DF-ESR	18
7.1 ± 1.0	18^{+9}_{-6}	2330 ± 121	240-460	FP-RA	16
5.8 ± 0.3				FP-RA	15
6.97 ± 0.70	5.9	2009 ± 151	298-424	FP-RF	19
6.08 ± 0.37	4.9 ± 0.5	1990 ± 340	250-396	FP-RF	this work[c]

[a] FP-RA = flash photolysis-resonance absorption. DF-ESR = discharge flow-electron spin resonance. FP-RF = flash photolysis-resonance fluorescence. DF-RF = discharge flow-resonance fluorescence. [b] Observed curved ln k vs. $1/T$ plots, and hence did not report E/R values. [c] This expression has been derived from only the low-temperature data.

rates were measured at several (minimum four, on the average six) fixed reactant concentrations. The bimolecular reaction rate constant was obtained from the slope of the k' vs. reactant concentration plots. Figure 3 shows one such plot for k_2 at 932 K. The measured values of k_1 and k_2 at various temperatures are listed in Tables I and II, respectively. The quoted errors are 2σ and represent the precision of the measured rate coefficient. It is estimated that the accuracy (2σ) of the rate constant at 298 K is ~15% and that it decreases to ~25% as the temperature is either raised to 1000 K or lowered to 250 K. The main source of estimated systematic error is in the knowledge of the concentration of H_2 and D_2 at the given temperature. (Note: This includes the error in the measured temperature and possiblity of impurity reactions at low temperatures.)

It has been previously shown that under our experimental conditions radical–radical reactions such as H + OH or OH + OH are insignificant.[11] To ensure that our present results were free from such secondary reactions, $[OH]_0$, the flash energy, $[H_2O]$, and the system pressure were varied at most temperatures. The results indicated the absence of any secondary reactions contributing to the measured values of k_1 and k_2.

The values of k_1 and k_2 are very small at low temperatures. Therefore, very small concentrations of reactive impurities—on the order of 1 ppm—could contribute significantly to the measured [OH] decay rates. Although it is always difficult to rule out completely the possibility of impurity reactions, our samples of H_2 and D_2 were known to have been very pure. Both H_2 and D_2 contained less than 1 ppm of CH_4 (according to the analysis by the gas company), the only organic species present in measurable quantities. Care was taken to ensure that no impurities were added in the course of transferring H_2 and D_2 from the tanks to the reactor. (It is easy to show that, to get 20% contribution from impurity reactions to the lowest rate constant which we measured, it is necessary to have as much as 6 ppm of an impurity which reacts with OH with a rate coefficient of 1×10^{-11} cm^3 $molecule^{-1}$ s^{-1} (for example, C_2H_4) at 250 K.) Therefore, we believe that our values of k_1 and k_2 are accurate to better than 25% at 250 K.

Figure 4 shows plots of ln k_1 and ln k_2 vs. $1000/T$. Results of our previous measurements of k_1 in the temperature range of 298–992 K are also included. It is clear that the Arrhenius plots are nonlinear for both reactions; ln k_2 vs. $1000/T$ seems to be more nearly linear than ln k_1 vs. $1000/T$. We have fitted our previously measured k_1 values between 298 and 992 K, using a nonlinear least-squares program, to the function $k_1(T) = (4.12 \times 10^{-19})T^{2.44} \exp(-1281/T)$ cm^3 $molecule^{-1}$ s^{-1}, while Zellner,[2]

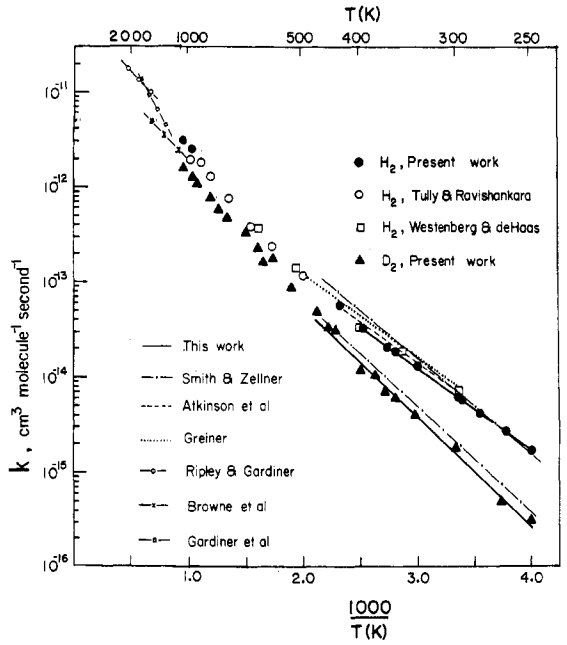

Figure 4. Plots of ln k_1 and ln k_2 vs. $1000/T$. For the sake of clarity, individual error bounds are not shown. (O) k_1 values from ref 8; (□) k_1 values from ref 18. Arrhenius parameters reported by previous investigators are as follows: (–·–) Smith and Zellner, ref 16; (– – –) Atkinson et al., ref 19; (···) Greiner, ref 17; (–O–) Ripley and Gardiner, ref 21; (–X–) Brown et al., ref 23; (–□–) Gardiner et al., ref 22; (—) Arrhenius fit to low-temperature data from this work.

using all previous measurements, obtained $k_1(T) = (1.66 \times 10^{-16})T^{1.6} \exp(-1660/T)$ cm^3 $molecule^{-1}$ s^{-1}. Our present data are best described by the former of these two expressions. A similarly derived three-parameter expression for reaction 2 based solely on our data yields the rate coefficient expression $k_2(T) = (4.37 \times 10^{-15})T^{1.18} \cdot \exp(-2332/T)$ cm^3 $molecule^{-1}$ s^{-1}.

Discussion

Reaction 1 has been studied by numerous investigators[12-15] at room temperature. In addition, there are four studies of k_1 as a function of temperature.[16-19] With one

(12) F. Kaufman and F. P. delGreco, *Discuss. Faraday Soc.*, **33**, 128 (1962).
(13) G. Dixon-Lewis, W. E. Wilson, and A. A. Westenberg, *J. Chem. Phys.*, **44**, 2877 (1966).
(14) F. Stuhl and H. Niki, *J. Chem. Phys.*, **57**, 3171 (1972).
(15) R. Overend, G. Paraskevopoulos, and R. J. Cvetanovic, *Can. J. Chem.*, **53**, 3374 (1975).
(16) I. W. M. Smith and R. Zellner, *J. Chem. Soc., Faraday Trans. 2*, **70**, 1045 (1974).
(17) N. R. Greiner, *J. Chem. Phys.*, **51**, 5049 (1969).

TABLE IV: Summary of Rate-Constant Data for Reaction 2, OH + D_2 → DHO + D

$k_2(298) \times 10^{15}$, cm^3 $molecule^{-1}$ s^{-1}	$10^{11}A$, cm^3 $molecule^{-1}$ s^{-1}	E/R, K	temp range, K	technique[a]	ref
2.1 (±12.5%)				FP-RA	24
2.05 ± 0.31				FP-RF	14
2.2 ± 0.4	$1.25^{+0.6}_{-0.4}$	2598 ± 182	210–460	FP-RA	16
2.11 ± 0.18				FP-RA	25
1.83 ± 0.12	1.21 ± 0.52	2671 ± 147	250–470	FP-RF	this work

[a] FP-RA = flash photolysis–resonance absorption. FP-RF = flash photolysis–resonance fluorescence.

exception,[18] all previous studies had an upper temperature limit of 500 K. Table III lists the 298 K values and, where appropriate, the Arrhenius parameters obtained by other investigators. There exists reasonable agreement among various k_1 (298 K) values. As pointed out earlier, the ln k_1 vs. $1000/T$ (Arrhenius) plot is nonlinear. For the sake of comparison, however, we have fitted our low-temperature ($T < 400$ K) (ln k vs. $1/T$) data to a linear Arrhenius expression obtaining

$$k_1(T) = (4.9 \pm 0.5) \times 10^{-12} \exp\{-(1.99 \pm 0.34) \times 10^3/T\} \text{ cm}^3 \text{ molecule}^{-1} \text{ s}^{-1}$$

where the errors are 2σ and $\sigma_A \equiv A\sigma_{\ln A}$. These values are listed in Table III. Our values of A and E/R are in good agreement with other determinations except that of Smith and Zellner.[16] These authors were the only investigators who measured k_1 at $T < 298$ K. They encountered some difficulty at temperatures below 270 K as secondary reactions such as

$$OH + OH + M \rightarrow H_2O_2 + M \quad (3)$$

or

$$OH + H + M \rightarrow H_2O + M \quad (4)$$

contributed to their measured [OH] temporal profiles. Corrections were made to take into consideration the contributions of these secondary reactions. Figure 4 presents the Arrhenius lines reported by Greiner,[17] Smith and Zellner,[16] and Atkinson et al.[19] Below 298 K our individual data points are fairly well represented by the line of Smith and Zellner; above 298 K they show good agreement with the results of the other investigators. It is particularly interesting to note the agreement over the entire temperature range of our results with those of Westenberg and deHaas,[18] the first investigators to notice the nonlinear variation of ln k_1 with $1000/T$.

In addition to the above-mentioned direct determinations, $k_1(T)$ has been calculated from flame and shock-tube data at temperatures above 1000 K.[20] For comparison with the present study, results of a few selected studies are shown in Figure 1. As seen from Figure 4, the shock-tube studies of Ripley and Gardiner[21] and Gardiner et al.[22] are in good agreement with the extrapolations of the present results, while the data of Browne et al.[23] seem to underestimate k_1 at $T > 1000$ K. The results of shock-tube studies in conjunction with our results (which together cover a temperature range 250–2600 K) clearly show the curvature in the Arrhenius plot.

Reaction 2 has been studied at 298 K by three groups.[14,24,25] The temperature dependence of k_2 has been previously studied only by Smith and Zellner.[16] Table IV lists all available data on reaction 2. Again, for the sake of comparison, we have fitted our low-temperature data ($T < 470$ K) to an Arrhenius form and obtained the A and E/R values shown in Table IV. There is reasonable agreement among all measured values of k_2 (298 K), our value being the smallest. Furthermore, the Arrhenius expression derived in this study, $k_2(T) = (1.21 \pm 0.52) \times 10^{-11} \exp\{(-2.67 \pm 0.15) \times 10^3/T\}$ cm^3 $molecule^{-1}$ s^{-1}, agrees well with that of Smith and Zellner.[16]

One of the main aims of this work was to obtain a set of data using a single technique over a wide temperature range for related reactions such that a coherent data base would be available to compare present-day theory with experimental results. Based on our data, two qualitative observations may be made: (1) the ln k vs. $1/T$ plots are nonlinear for both reactions 1 and 2; and (2) the magnitude of the kinetic isotope effects, i.e., k_1/k_2, increases with decreasing temperature. Comparison of experimental results with theory may be made at different levels of quantification. The general nonlinear Arrhenius behavior for bimolecular reactions can be qualitatively explained, and is even to be expected, on the basis of chemical kinetic theories of elementary reactions. Zellner[2] and Gardiner[3] have recently discussed the probable causes for this behavior in terms of transition-state theory and/or collision theory.

The transition-state theory can be used at many levels of rigor to calculate the values of $k_1(T)$ and $k_2(T)$ (and hence $k_1(T)/k_2(T)$). Assuming a transition-state structure, one can predict the temperature variation of the bimolecular rate coefficient k quite well when the transition-state properties are forced to reproduce the value of k measured at one temperature. Recently, however, ab initio potential energy surfaces have been calculated for simple atom–diatom reactions and even four-atom reactions such as reactions 1 and 2.[7] Using the calculated potential energy surface, conventional transition-state theory calculations have been carried out by Schatz and Walch[5] and Isaacson and Truhlar[26] for reaction 1 and by Schatz and Wagner[27] and Isaacson and Truhlar[26] for reaction 2. Isaacson and Truhlar[26] have also calculated $k_1(T)$ and $k_2(T)$ based on canonical variational theory. Figure 5 shows the calculated values of $k_1(T)$ based on conventional transition-state theory which includes and excludes tunneling as well as canonical variational theory which excludes tunneling. Very similar results are obtained for reaction 2. It is clear

(18) A. A. Westenberg and N. deHaas, *J. Chem. Phys.*, 58, 4061 (1973).
(19) R. Atkinson, D. A. Hansen, and J. N. Pitts, Jr., *J. Chem. Phys.*, 63, 1703 (1975).
(20) G. Dixon-Lewis and D. J. Williams, *Compr. Chem. Kinet.*, 17, 1–248 (1977).
(21) D. L. Ripley and W. C. Gardiner, Jr., *J. Chem. Phys.*, 44, 2285 (1966).
(22) W. C. Gardiner, Jr., W. G. Mallard, M. McFarland, K. Morinaga, J. H. Owen, W. T. Rawlins, T. Takeyama, and B. F. Walker, *Symp. (Int.) Combust., [Proc.]*, 14, 61 (1973).
(23) W. G. Browne, R. P. Poster, J. D. Verlin, and A. K. Clarke, *Symp. (Int.) Combust., [Proc.]*, 12, 1035 (1966).
(24) N. R. Greiner, *J. Chem. Phys.*, 48, 1413 (1968).
(25) G. Paraskevopoulos and W. S. Nip, *Can. J. Chem.*, 58, 2146 (1980).
(26) A. Isaacson and D. G. Truhlar, private communications, 1980.
(27) G. Schatz and A. Wagner, private communications, 1980.

TABLE V: Comparison of the Experimentally Measured Kinetic Isotope Effect ($k_1(T)/k_2(T)$) with Calculated Values

		ref 16		ref 5 and 27,	ref 26		
temp, K	exptl result[a]	BEBO	LEPS	$\neq$/W[d]	$\neq$[c]	$\neq$/W[d]	CVT[e]
250	5.4 ± 1.5			8.9	3.6	5.6	2.2
298	3.3 ± 0.9	3.6	3.7	7.0	3.3	4.9	2.2
400	2.5 ± 0.7[b]			4.3	2.9	3.9	2.1
600	1.7 ± 0.5[b]			3.3	2.3	2.8	2.0
1000	1.6 ± 0.5[b]			2.3	1.8	2.0	1.7

[a] The quoted errors are ~30%, which is calculated on the basis of the estimated accuracy of $k_1(T)$ and $k_2(T)$. [b] Since both $k_1(T)$ and $k_2(T)$ were not measured at exactly these temperatures, the three-parameter equations given in the text were used to calculate $k_1(T)$ and $k_2(T)$. [c] $\neq$ denotes transition-state theory using the potential energy surface calculated by Walch and Dunning (ref 7). [d] $\neq$/W denotes transition-state theory using Wigner tunneling correction based on the potential energy surface calculated by Walch and Dunning (ref 7). [e] CVT = canonical variational theory (excluding tunneling) using the potential energy surface calculated by Walch and Dunning (ref 7).

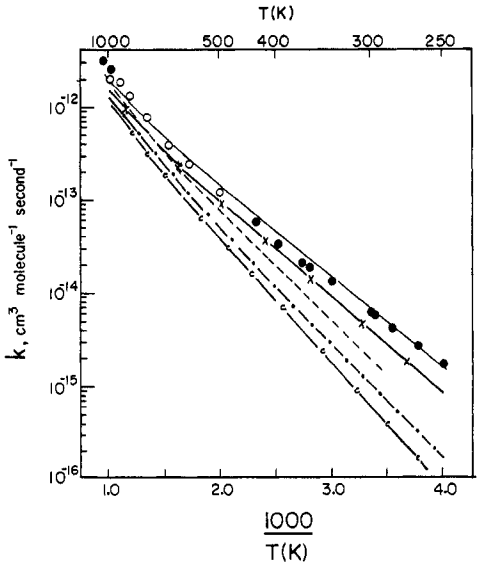

Figure 5. Comparison of experimental values of $k_1(T)$ with calculations carried out by using the ab initio surface of Walch and Dunning, ref 7: (—) TST calculation including tunneling correction (Schatz and Walch, ref 5); (– – –) TST calculation excluding tunneling (Schatz and Walch, ref 5); (–X–) TST calculation including tunneling correction (Isaacson and Truhlar, ref 26); (–•–) TST calculation excluding tunneling (Isaacson and Truhlar, ref 26); (–c–) canonical variation theory calculation excluding tunneling (Isaacson and Truhlar, ref 26).

from Figure 5 that calculated $k_1(T)$ values are much lower than experimental values when tunneling is neglected, the discrepancy increasing with decreasing temperature. The differences in the numerical values obtained by two sets of calculations[26,27] are due to the exact choices of input parameters and will be discussed by those authors in forthcoming publications. The canonical variational theory calculations which exclude tunneling yield the lowest calculated values for both $k_1(T)$ and $k_2(T)$. In fact, the difference between the calculated and measured values of $k_1(T)$ at 250 K is about a factor of 20. It is expected, however, that inclusion of tunneling would greatly enhance the agreement between the calculations and the experimental results, as was observed for the reaction of Cl with H_2. In this reaction, the calculated tunneling correction to the canonical variational theory at 245 K is a factor of 4.0.[6] It should be pointed out that small errors in the calculated barrier heights could significantly change the absolute value of $k_1(T)$ and $k_2(T)$ at a given temperature without drastically changing the shape of the Arrhenius curve. However, since such an error would have the maximum effect on $k_1(T)$ at low temperature, it is hard to separate this effect from errors in tunneling calculations. In spite of this possibility, it can still be said that all of these calculations suggest that tunneling is a major contributor to the overall rate coefficient for the reaction and that the tunneling contribution increases quite dramatically with decreases in temperature.

Another experimental parameter which may be compared with the theoretical calculations is the magnitude of the kinetic isotope effect, k_1/k_2. Table V lists these values for the cases considered above and for the calculations of Smith and Zellner. Smith and Zellner[16] used two different semiempirical surfaces, i.e., LEPS and BEBO, and they neglected tunneling. They assumed that the energy barrier height is the same as the experimentally measured activation energy. It is clearly seen that all calculations show the observed trend in k_1/k_2, i.e., a decrease with increase in temperature. Moreover, it is interesting to note that the best agreement between measured and calculated values of k_1/k_2 is obtained when tunneling is neglected. Even in the case of the semiempirical calculations of Smith and Zellner, there is good agreement between measured and calculated kinetic isotope effects. However, in spite of the good agreement in isotope effect ratios, the absolute values of k_1 and k_2 are grossly underestimated when tunneling is neglected.[5,26,27] It is interesting to note that, while the TST calculations which exclude tunneling overestimate k_1/k_2 at $T > 298$ K, the canonical variational theory underestimates this ratio. Therefore, it is quite likely that inclusion of a tunneling correction would bring the calculations of the canonical variational theory treatment into better agreement with experimental results.

It is worth inquiring what experimental work can be carried out to further check and aid in the calculation of the elementary reaction rate coefficients. Two experiments are suggested: (a) extension of measurement of k_1 and k_2 to temperatures much lower than 250 K where tunneling should dominate and to temperatures higher than 1000 K where energetics are less important; (b) measurement of rate coefficients for the reaction of OH with HD. Since the same potential energy surface that is used for H_2 and D_2 will be applicable, it will be interesting to see whether the theory can predict the measured thermal rate coefficients for the reaction of OH with HD. Both of these experiments will be underway shortly in our laboratory.

Acknowledgment. This work was supported by the Air Force Office of Scientific Research under Contract No. F49620-77-C-0111. We are greatly indebted to Professors D. Truhlar and G. Schatz and to Dr. A. Wagner for providing us with their calculations on k_1 and k_2 as well as many helpful suggestions. We thank Dr. P. H. Wine for helpful discussions throughout the course of this work.